PHILOSOPHICAL TRANSACTIONS B

royalsocietypublishing.org/journal/rstb

Review

Cite this article: Rauzi M. 2020 Cell intercalation in a simple epithelium. *Phil. Trans. R. Soc. B* **375**: 20190552.
http://dx.doi.org/10.1098/rstb.2019.0552

Accepted: 2 March 2020

One contribution of 15 to a discussion meeting issue 'Contemporary morphogenesis'.

Subject Areas:
cellular biology, developmental biology, biomechanics

Keywords:
junction remodelling, actomyosin tension, E-cadherin adhesion, actomyosin flow

Author for correspondence:
Matteo Rauzi
e-mail: matteo.rauzi@univ-cotedazur.fr

THE ROYAL SOCIETY PUBLISHING

Cell intercalation in a simple epithelium

Matteo Rauzi

Université Côte d'Azur, CNRS, Inserm, iBV, Nice, France

MR, 0000-0002-6313-0668

Cell intercalation is a key topological transformation driving tissue morphogenesis, homeostasis and diseases such as cancer cell invasion. In recent years, much work has been undertaken to better elucidate the fundamental mechanisms controlling intercalation. Cells often use protrusions to propel themselves in between cell neighbours, resulting in topology changes. Nevertheless, in simple epithelial tissues, formed by a single layer of densely packed prism-shaped cells, topology change takes place in an astonishing fashion: cells exchange neighbours medio-laterally by conserving their apical–basal architecture and by maintaining an intact epithelial layer. Medio-lateral cell intercalation in simple epithelia is thus an exemplary case of both robustness and plasticity. Interestingly, in simple epithelia, cells use a combinatory set of mechanisms to ensure a topological transformation at the apical and basal sides.

This article is part of the discussion meeting issue 'Contemporary morphogenesis'.

1. Introduction

A fascinating feature of cells, in epithelia sheets, is their capacity to change topology: topology change occurs when a cell loses or gains new contact with neighbouring cells. One important topological change is cell intercalation (referred to as type 1 transition, T1, in foam physics). Intercalation results from the gain of new contact between two or more cells and the eventual complete loss of contact between adjacent cells, leading to cell neighbour exchange (i.e. cell rearrangement). Gain and complete loss of contact are inextricable in an imaginary 2D space (figure 1*a*, from (ii) to (iii)) but not in the real 3D space, where new contact gain between two cells can occur without complete loss of contact with neighbouring cells (figure 1*b*, from 1. to 3.).

Cell intercalation has been shown to play a key role in both tissue homeostasis and morphogenesis. For instance, cell rearrangement ensures tissue homeostasis in more mature epithelia that do not undergo extensive remodelling, forming robust barriers. Mature epithelia can be subject to stresses caused by intrinsic (e.g. cell division and cell delamination) and extrinsic (boundary condition variations) forces. Cell intercalation plays the role of stress releaser by providing the fluidity required to ensure tissue integrity [1]. Under these conditions, cell neighbour exchange is not polarized, can be reversible, has no effect on global or local shape and is driven by stochastic local fluctuations of the cell cytoskeleton, and it is predicted to eventually decrease local topological disorder [1,2].

Cell intercalation has been shown to also play an important role in competitive environments. For instance, in cell crowding conditions, cell neighbour exchange can facilitate cell extrusion [3], while during cell invasion, it promotes winner–loser cell contact increase, which can lead to loser cell apoptosis [4].

Cell intercalation is a key process during embryonic epithelial morphogenesis and more specifically during embryo gastrulation. To drive tissue shape changes, intercalation has to be (i) polarized to orient tissue deformation and (ii) irreversible to impose morphogenetic progression resulting in a net displacement of cellular masses driving local, and eventually global, tissue shape changes. While intercalation polarity is a key morphogenetic driver, recent studies have shown that non-polarized cell neighbour exchange can also promote epithelial morphogenesis. During chick gastrulation, stochastic cell rearrangements, mediated by cell division in tandem with primitive streak contraction, favour polarized rotatory

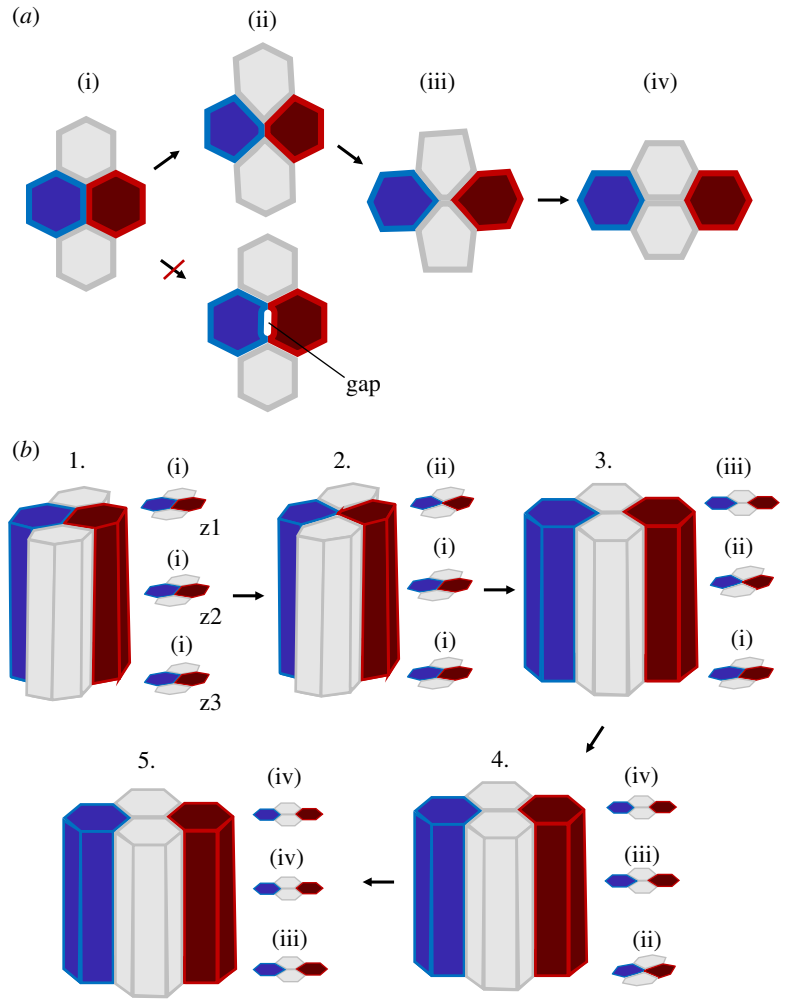

Figure 1. Cell intercalation in 2D and 3D. (*a*) Two-dimensional representation of cell intercalation. During intercalation a junction shrinks and a new junction forms and extends. During this process no gaps are formed. (*b*) Three-dimensional representation of cell intercalation. Cells start to intercalate from one end (e.g. from the apical side) forming scutoid shapes. Cell neighbour exchange then propagates from one end to the other, resolving cell intercalation. (Online version in colour.)

cell flows (i.e. 'Polonaise movements') [5]. This supports the idea that stochastic cell intercalation can function as a tissue fluidizing process not only during tissue homeostasis but also during morphogenesis, eventually preventing cell jamming [6,7].

Cells can rearrange in different ways. In simple epithelia (tissue constituted by a single cellular layer), cells can intercalate medio-laterally: cell rearrangement occurs within the plane of the epithelium. Planar polarized medio-lateral intercalation promotes tissue convergence and extension. One exemplary case is the convergence–extension of the *Drosophila* embryo germband during gastrulation [8]. If intercalation polarity is centrosymmetric, medio-lateral cell rearrangement can also facilitate tissue folding: a classic example is archenteron elongation in the gastrulating sea urchin embryo [9] or, as presented in a much more recent study, salivary gland tube formation in the *Drosophila* embryo [10]. Polarized cell intercalation associated with planar cell-shape chirality can instead facilitate tissue rotation, for instance during genitalia development in the *Drosophila* pupa [11]. In multi-stratified epithelia, cells can intercalate radially: cells belonging to one layer rearrange with cells of a second layer driving extension in the plane of and thinning along the axis perpendicular to the multi-stratified epithelium [12–14]. A review by Walck–Schannon & Hardin comprehensively presents the different modes of cell rearrangement [15].

The remainder of this review will focus on the process of cell intercalation in simple epithelia constituted by apico-basal polarized cells, highlighting our present understanding of how medio-lateral cell neighbour exchange is initiated and how it eventually resolves.

2. Initiating intercalation: establishing cell–cell contacts

Cell intercalation begins with the remodelling of a cell–cell contact, which eventually leads to contact loss (figure 1*a*). In order to remodel a contact, it is necessary that contact between cells is established so that cells can initially adhere one another. In the absence of cell–cell adhesion (e.g. if cells are packed together but do not form contacts) intercalation cannot be initiated. Cellular adhesion can be mediated, for instance, by adherens junctions, which are known to play a key role in cell–cell coupling and force transmission [16,17]. Adherens junctions, in simple epithelia, are usually located at the cell subapical region and are formed by cadherins (e.g. E-cadherins), which are transmembrane homophilic proteins. While cadherins interact extracellularly with each other, they interact with the actomyosin cytoskeleton intracellularly via the alpha and beta subunits [18–22]. The establishment of cell–cell adherens junctions is thus a necessary condition to initiate junction remodelling.

3. Initiating intercalation: losing cell contact

Once cells have adhered to one another, how can adherens junctions be remodelled to drive contact loss? Interestingly, a contact junction between four intercalating cells usually reduces in size without forming gaps in the tissue (figure 1*a*(ii) bottom). Junction size reduction is often referred to as junction 'shrinking' or 'shortening'; while these expressions are on one hand simplistic (i.e. do not refer to a precise mechanism driving junction remodelling and can thus be misleading), on the other they are simple, thus appealing to provide an intuitive description of the first phase of cell intercalation (figure 1*a*, from (i) to (ii)). Apical junction shrinkage initiating cell intercalation has been reported in multiple embryo model systems, such as, as for instance, in chick [23,24], in *Xenopus laevis* [25], in mice [26] and in *Drosophila* [27]. In this review, I will mainly refer to the *Drosophila* model system, where the process of junction shrinking has been best characterized and studied.

(a) Cortical tension anisotropy

Studies focused in understanding cellular packing and tissue remodelling in the *Drosophila* model system were the first attempts to shine new light on the process of junction shrinkage [28–30]. In these studies, the authors applied the physical concept of surface tension (line tension) to cell–cell junctions. Cell surface tension is the amount of energy required to increase the cell surface of a unit area. Increasing actomyosin contractility increases surface tension, while increasing E-cadherin-based adhesion lowers surface tension between two cells, eventually driving cell–cell contact reduction and increase, respectively [16]. During germband elongation in the early developing *Drosophila* embryo, proteins controlling surface tension are distributed in a planar cell polarized fashion: while junctions parallel to the dorsal–ventral (DV) axis of the embryo have higher levels of myosin II and lower levels of E-cadherin (favouring higher surface tension), junctions parallel to the anterior–posterior (AP) axis present lower levels of myosin II and higher levels of E-cadherin (favouring lower surface tension) [31–34]. Tension anisotropy between AP and DV junctions could initiate cell intercalation by driving shrinkage of junctions under higher tension (i.e. parallel to the DV axis). Higher tension along junctions parallel to the DV axis was demonstrated using subcellular laser dissection to selectively disrupt the actomyosin cortical network at different junctions; tension was probed by measuring vertices' (end points of a junction where three cells meet) maximum recoil speed [30]. Cortical tension anisotropy driven by the polarized distribution of actomyosin contractility is the first model to provide new understanding of how cell junctions can be remodelled to initiate cell intercalation (figure 2*a*).

(b) Periodic actomyosin contractions

Periodic actomyosin contractions were reported for the first time in the seminal study by Munro *et al*. in 2004 in the *C. elegans* single-cell embryo [37]. These contractions result from the local (few micrometres in diameter) coalescence of the actomyosin network within less than a minute. Since actomyosin periodic contractions are the result of a sudden and local density increase and eventual decrease of filamentous actin (F-actin) and myosin II (Myo II), these contractions are also referred to as 'pulses'. When F-actin and Myo II are monitored with a fluorescent probe (e.g. eGFP), pulses result from the sudden increase and eventual decrease of signal intensity. Since the seminal work by Munro and colleagues, actomyosin pulses have been reported in numerous studies focused on understanding the underlying mechanisms responsible for cell shape change and tissue morphogenesis during embryo development [35,38–41]. While a large body of *in vivo*, *in vitro* and *in silico* evidence has recently elucidated the nature and the origin of the actomyosin pulses [42–47], here I will focus more specifically on the role of pulses in cell intercalation.

During cell intercalation in the prospective ectoderm of the early–*Drosophila* embryo, actomyosin pulses form in the apical–medial region of cells, flow towards the junctional cortex and eventually fuse with the junctional actin network. Actomyosin material is thus transferred from the medial to the junctional cell region. By monitoring junction shrinkage during cell intercalation at high temporal resolution, Rauzi *et al*. [35] showed that junctions shrink in a stepwise fashion: alternating shrinking and stalling phases occur several times before complete contact junction loss. Shrinking phases correlate with pulse formation and flow towards the junctional cortex. By specifically disrupting actomyosin pulses using highly resolved laser dissection, junction shrinkage is hampered. Finally, while medial actomyosin pulsation and flow drive junction shrinkage, junctional actomyosin (partially resulting from the flow and fusion of the medial actomyosin pulses with the junctional actin cortex) stabilizes junction length after shrinkage (figure 2*b*).

Pulse flow from the medial to the junctional region of the cell is thus a crucial process to drive junction shrinkage. How is medial actomyosin flow oriented? Actin and actomyosin networks can exert traction forces orienting the flow towards regions with higher anchorage [48,49]. Nevertheless, actomyosin pulses flow towards shrinking junctions that have less E-cadherin (i.e. fewer anchoring sites) [32,34]; this is a striking paradox. Interestingly, the levels of E-cadherin at shrinking junctions periodically fluctuate over time scales that are comparable to actomyosin pulse formation time periods [35,49]. Levayer & Lecuit in 2013 tried to solve this paradox, proposing a model in which the medial actomyosin network flows along directions with higher anchorage imbalance and towards junctions with higher levels of E-cadherin (figure 2*c*). This model only partially solves the paradox since (i) medial actomyosin flow precedes (i.e. cannot be the consequence of) junctional E-cadherin sudden increase [35,49] and reinforcement [50] at shrinking junctions, and also because (ii) medial actomyosin flow follows E-cadherin sudden decrease at the shrinking junctions [35]. Interestingly, recent work by Pinhero and colleagues in 2017 showed that actomyosin flows are triggered by local downregulation of E-cadherin at the cytokinetic furrow during cell division. Flow is proposed to be triggered by local actomyosin network fluidization [51]. Local F-actin fluidization could also take place in a zone close to shrinking junctions following the rapid and periodic decrease of E-cadherin, which would facilitate and eventually direct medial actomyosin flow. Additional work is necessary to further elucidate the mechanisms triggering actomyosin medial flow direction driving junction shrinkage.

(c) Vertex sliding

Vanderleest and colleagues in 2018 proposed a new model for contact junction remodelling based on vertex 'sliding' [52]. The authors carefully monitored vertex displacement during cell

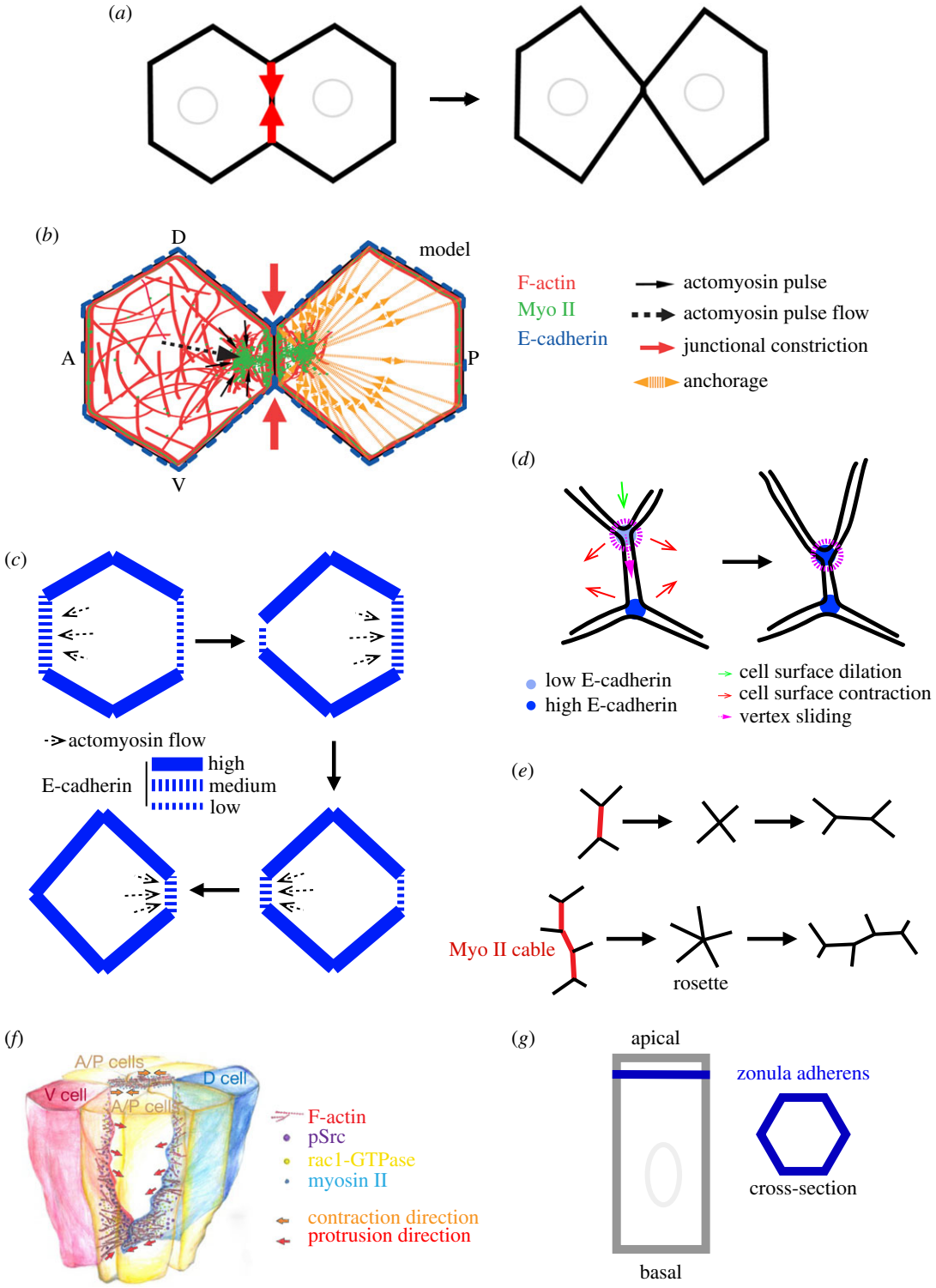

Figure 2. Mechanisms driving junction shrinkage. (*a*) Cortical tension model for junction shrinkage. (*b*) Medial actomyosin contraction model for junction shrinkage. Adapted with permission from Rauzi *et al.* [35]. (*c*) Differential anchorage model for actomyosin pulse flow. (*d*) Vertex sliding model for junction shrinkage. (*e*) Representation of a fundamental and a rosette intercalation event. (*f*) Basal–lateral protrusion model for cell intercalation initiation. Adapted with permission from Sun *et al.* [36]. (*g*) Representation of a columnar epithelial cell.

intercalation in the prospective *Drosophila* ectoderm. Interestingly, the change of one vertex position at one end of a shrinking junction does not often correlate with the mirrored change in position of the vertex at the other end. In addition, when the position of one vertex shared by two junctions (e.g. a shortening junction parallel to the DV axis and a junction parallel to the AP axis) changes, while one junction shortens (e.g. the junction parallel to the DV axis), the other (e.g. the junction parallel to the AP axis) concomitantly lengthens, such that the overall contact length remains constant (figure 2*d*). These striking observations suggest that a vertex-specific mechanism could be at play controlling vertex position during contact junction shortening. The authors refer to the change of vertex position as vertex 'sliding'; this expression, while simplistic, is appealing in that it provides an intuitive description of the process. Vanderleest and colleagues report that vertices slide in a stepwise fashion and that their displacement correlates with fluctuations of E-cadherin at vertices. Low E-cadherin levels correlate with vertex sliding onset, while high E-cadherin levels correlate with vertex stalling. When constant high E-cadherin levels

are maintained (e.g. by inhibiting endocytosis), the vertex position persistently stalls and cell intercalation is compromised [34,52]. Levels of E-cadherin thus play a key role in vertex sliding and contact junction remodelling: low E-cadherin levels are necessary to initiate junction shortening (in agreement with previous work [35]), while high E-cadherin levels stabilize contact junction length between intercalating cells. Myo II is enriched at vertices a few seconds prior to E-cadherin enrichment (in agreement with previous studies monitoring junctional E-cadherin fluctuations [35,49]). Increased E-cadherin levels at vertices could be driven by local medial actomyosin contractions focusing E-cadherin proteins tethered to F-actin networks [47,53].

The work of Vanderleest and colleagues strongly supports the idea that vertices are not just geometric entities. Vertices could constitute molecular hubs disassembling junctions at the 'front' (shrinking the junctions parallel to the DV axis) and reassembling junctions at the 'rear' (lengthening the junctions parallel to the AP axis).

Vanderleest and colleagues also reported that cell surface area fluctuates over time as a consequence of medial actomyosin contractions. By using cross-correlation analysis, the authors show that efficient vertex sliding is achieved when two of the three cells sharing the vertex contract their surface area, while the third cell simultaneously dilates its surface area (figure 2*d*). The mechanism responsible for polarized vertex sliding (e.g. along the DV axis) remains elusive. One hypothesis is that vertex sliding is facilitated along junctions parallel to the DV axis while it is impaired along junctions parallel to the AP axis that have low and high levels of E-cadherin, respectively [32,34]. A second hypothesis invokes an emerging supracellular mechanism. For instance, synchronized area contraction of anterior and posterior cells, together with the dilation of dorsal and ventral cells of an intercalating quartet, could be more frequent than other possible contraction/dilation combinations. A third hypothesis is that the 'vertex sliding' model complements the previously described 'periodic actomyosin contraction' and the 'cortical tension anisotropy' models. Further work is necessary to better understand how seemingly different models for the same process are compatible and can eventually complement each other.

(d) Rosette formation

Medio-lateral cell intercalation in simple epithelial tissues generally occurs among four cells (i.e. the fundamental intercalating unit). Nevertheless, intercalating units of more than four cells have also been reported and referred to as rosettes (figure 2*e*) [24,25,54,55]. Rosettes are also driven by actomyosin cortical tension [30,56] and contribute to convergence extension in a way that is equivalent to the additive effects of multiple individual fundamental intercalation units [57]. Rosettes result from the contraction of aligned and juxtaposed junctions enriched in actomyosin, which are referred to as 'cables' (figure 2*e*) [54]. A recent study by Paré and colleagues reported that the ectopic striped expression of Toll receptors can induce actomyosin cable formation in the prospective ectoderm of the *Drosophila* embryo [58]. It would be interesting in the future to further investigate the origin of cables in intercalating units of more than four cells.

(e) Basal–lateral protrusions

Basal–lateral protrusion is another mechanism bringing two cells in proximity to one another. Basal–lateral protrusion is reported during dorsal midline formation in *Caenorhabditis elegans* [59–62] and during notochord primordium formation in *Ciona intestinalis* [63–66]. Cell protrusion directs cell motility similarly to what is reported for non-epithelial cells [67]. A more recent study by Sun and colleagues in 2017 reports basal–lateral cell protrusion formation in tandem with apical junction remodelling [36]. By using two-photon live imaging, the authors monitored intercalating cells in the *Drosophila* prospective ectoderm at a more basal position of rosettes (figure 2*e*). Sun and colleagues reported that F-actin-enriched protrusions form in more dorsal and ventral cells of rosettes 15–20 µm from the apical surface. Protrusions are polarized along the DV axis of the embryo and point towards the centre of the rosette (figure 2*f*). By using one-photon activation optogenetics, the authors showed that basolateral protrusions are Rac1-dependent. The tyrosine kinase Src42A was identified as a factor upstream of Rac1 that specifically affects basal–lateral protrusion. While apical rosette formation is driven by actomyosin cortical tension [30,56], basal rosette formation is mainly driven by Rac1-dependent protrusions. Both apical and basal rosette formation contribute to the extension of the prospective ectoderm. While this study suggests that the formation of apical and basal–lateral rosettes is mutually independent, further work is necessary to confirm this. For example, one could employ strategies to specifically perturb the basal–lateral or the apical machinery while monitoring the apical and basal cell sides, respectively. One such strategy is to implement two-photon activation optogenetics, which has been shown to be an effective technique to modulate protein concentration with spatial, temporal and protein specificity [68–70]. How is basal–lateral cell protrusion polarized? Sun *et al*. reported that basal rosettes are compromised in *eve* and *Toll-2*, *6*, *8* mutants. This suggests that the AP gene patterning could control protrusion polarity. What controls the direction of protrusion towards the centre of the rosette? Short-range signalling could control the direction of the protrusive activity similarly to what is observed during radial-cell intercalation in the *X. laevis* embryo, where cells extend under the control of short-range chemotaxis [71]. Further work is necessary to uncover the guiding signalling cues during basal–lateral rosette formation. This study shows that intercalation taking place in the *Drosophila* prospective ectoderm shares similarities with other medio-lateral intercalation processes in other model systems that are also mediated by cell protrusive activity [38,60,62,63,72]. The tyrosine kinase Src42A was already known to play a role in cell intercalation and, more specifically, in junction remodelling [73]. Cell–cell contact junctions are indeed also necessary during basal–lateral protrusion-based cell intercalation to mediate traction forces driving net cell displacement [74]. It remains to be conclusively determined if cell contact junctions are established and remodelled at the basal–lateral side of forming rosettes to mediate traction forces. Finally, Sun and colleagues proposed that basal–lateral intercalation mediated by cell protrusion could be a general intercalation mechanism taking place also in fundamental intercalating units (i.e. formed by four cells).

4. Initiating intercalation: gaining a new contact

While cell junction shortening is a process that has been studied extensively, few studies have tackled the question of how a new cell–cell contact subsequently lengthens (figure 1*a*, from (iii) to (iv)). While junction shortening is a necessary

condition for eventual new junction lengthening, Collinet and colleagues reported that junction shortening contributes 30% of the total extension of the intercalating quartet in the prospective *Drosophila* ectoderm. 70% of the extension then occurs during new junction lengthening [57]. Previous work had hypothesized that new junction lengthening could result from minimizing the energy of the tissue after junction shrinkage [30]. Under this hypothesis, tissue extension is a necessary condition for new junction lengthening. Collinet and colleagues challenged this hypothesis using genetic mutations and physical barriers to constrain the tissue and compromise its extension. Surprisingly, the number of new lengthening junctions in tissue-constrained conditions is equivalent to wild-type conditions. This shows that new junction lengthening (like junction shrinking) is an active cellular process.

What is the cellular mechanism driving new junction lengthening? A study by Yu & Fernandez-Gonzalez, using laser-based induced actomyosin accumulation, showed that medial actomyosin contraction in the anterior and posterior cells of an intercalating quartet is sufficient to drive new junction lengthening [75]. Pulsatile contractions of actomyosin continue to form in intercalating cells also during new junction lengthening. Collinet and colleagues showed that pulses of medial actomyosin correlate with phases of new junction lengthening occurring in a stepwise fashion. By using laser dissection, the authors finally demonstrated that medial actomyosin pulses drive new junction lengthening [57].

Interestingly, during the phase of junction lengthening, low density of E-cadherin is reported; E-cadherin at the new lengthening junction is diluted during the lengthening phase and gradually increases during the stalling phase [57]. This supports the idea that new junctions are gradually established between the dorsal and the ventral cells of the intercalating quartet. Actomyosin is strongly enriched in shrinking junctions but not in lengthening junctions. Bardet and colleagues reported that downregulation of the tumour suppressor PTEN in the developing *Drosophila* wing blade causes upregulation of Myo II in the newly forming junctions. This prevents new junctions from effectively lengthening and thus compromises cell intercalation [76]. The absence of high levels of actomyosin at the newly forming junctions is thus a necessary condition for new junction lengthening.

During the first phase of cell intercalation (figure 1*a*, from (i) to (ii)) actomyosin polarized flows play a key role in junction shrinkage. Flow polarization is thought to be driven by junctional E-cadherin polarized distribution [35,49]. During the second phase (figure 1*a*, from (iii) to (iv)), actomyosin pulses flow towards the newly formed junction, driving junction lengthening. In this second phase, after complete junction shrinkage, E-cadherin junctional distribution is no longer polarized. It is still not clear how medial actomyosin flow is oriented during new junction lengthening. Future work is necessary to test if actomyosin flow polarity is required for new junction lengthening and, if so, how polarity is controlled during this second phase of cell intercalation.

When a junction completely shrinks, the intercalating quartet reaches a critical configuration: this is referred to as the 'four way' junction since four cells seem to be in contact in a single punctate zone. This expression is nevertheless misleading. E-cadherin proteins can connect only two cells at a time, therefore dorsal–ventral cell adhesion and anterior-posterior cell adhesion are mutually exclusive within the zonula adherens. Recent work has proposed that the adhesion protein Sidekick, specifically localized at vertices, could play a role in cell intercalation [77,78] and more specifically during new junction formation [79]. This opens new avenues to better elucidate how the adhesive transition is taking place during this critical phase of cell intercalation (figure 1*a*, from (ii) to (iii)).

5. Resolving intercalation

An epithelial cell quartet (with apical, basal and lateral sides) initiates intercalation by remodelling the contact junctions: a junction shortens and disappears while a new junction forms and lengthens. Contact junctions are typically located in a subapical position called the *zonula adherens*: a cell contact band a few micrometres wide that encompasses the cell perimeter (figure 2*g*). As a consequence of junctional remodelling at the zonula adherens, cells change from a prism to a scutoid shape (figure 1*b*, from 1. to 3.). Scutoids are shapes that result from cells having different apical and basal neighbours. These shapes were initially described in a biological context by Condic and colleagues in 1991 [80] and then theoretically formalized by Gomez-Galvez and colleagues in 2018, who also coined the term 'scutoid' [81]. Scutoids have been theoretically predicted as steady state cell shapes formed especially in tubular structures providing mechanical stability. After junctional remodelling, cell neighbour exchange will resolve from apical to basal, completing cell intercalation. Since intercalation is usually not taking place simultaneously along the apical–basal axis and it is initiated at the zonula adherens, the process of intercalation results in a transition of cell shape from prism, to scutoid, to prism again (figure 1*b*). How do the cells transition from the scutoid to the prism shape (figure 1*b*, from 3. to 5.)? One possibility is that, while cortical forces initiate cell neighbour exchange at the zonula adherens, protrusions formed all along the lateral side could resolve cell intercalation (seemingly similar to what is reported during rosette formation [36]). Another possibility is that, after junctional remodeling at the zonula adherens, cells 'accommodate' apico-basally if this lowers the energy of the system. If cells have different sets of junctions (e.g. adherens junctions, septate junctions, gap junctions, etc.), all junctions along the apical–basal axis need to be remodelled to resolve cell intercalation. Future work is necessary to shine new light on the mechanisms responsible for cell shape remodelling from scutoid to prism resolving cell intercalation. Finally, 3D mathematical models capturing the apical–basal dynamics of resolving T1s are now necessary to help biologist unravel the key principles underlying this fundamental topological transformation.

6. Interplay between intercalation and external forces

Cell intercalation in epithelia is generally driven by cellular active mechanisms generating internal forces. This can be deduced in frog cultured explant showing convergence and extension movements mechanically independent of the rest of the embryo [82] or in sea urchin exogastrulae showing outward archenteron elongation [9]. Direct evidence of cell internal forces driving cell intercalation was reported in the

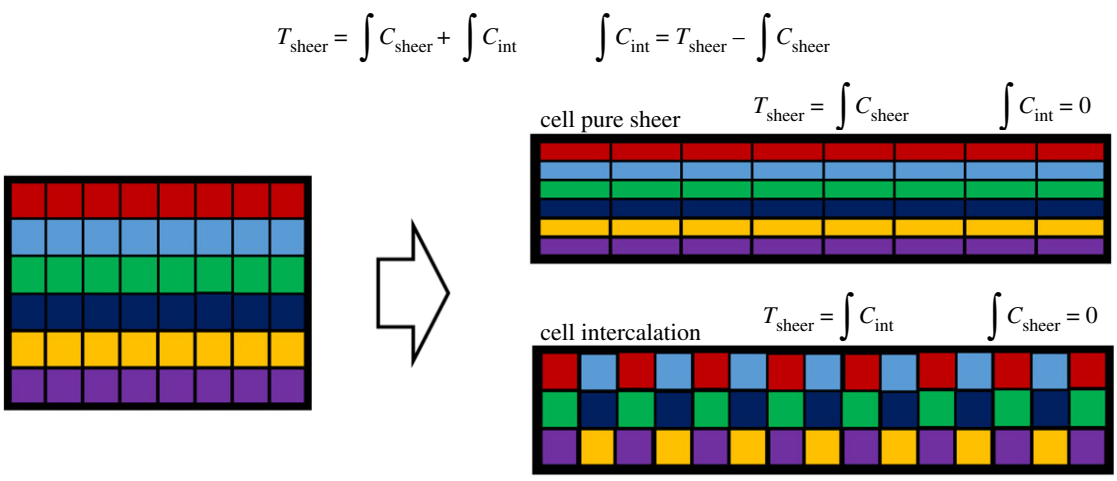

Figure 3. Contribution of cell intercalation to tissue pure shear. Tissue pure shear as a result of cell pure shear (top) or cell intercalation (bottom). (Online version in colour.)

Drosophila embryo (as presented earlier in this review). Nevertheless, during embryo development different tissues can interact, pushing and pulling on each other [40,83–85]. How do external mechanical forces impact on cell intercalation? A first answer to this question is provided by the work of Collinet and colleagues: if external forces are hampered at the boundary of the extending ectoderm tissue in the *Drosophila* embryo, the number of intercalation events is not reduced but the length and direction of newly extending junctions are altered [57]. This shows that compressive external forces can modulate intercalation shape and dynamics. In the early developing *Drosophila* embryo, the posterior midgut pulls on one end of the prospective ectoderm. Interestingly more intercalation events occur in the region of the ectoderm closer to the posterior end [58,86]. This suggests that pulling forces also could facilitate cell intercalation.

7. Measuring the contribution of cell intercalation to tissue convergence–extension

Polarized cell intercalation drives tissue convergence–extension. During convergence–extension, tissues undergo pure shear. Cell intercalation and cell pure shear contribute to tissue pure shear (figure 3). How can the contribution of cell intercalation to tissue pure shear be measured? Cell intercalation events can be measured by tracking and quantifying intercalation events in space and in time [58]. This can be achieved by tracking disappearing and newly forming interfaces or more simply by monitoring cell neighbour variations over time. Nevertheless, intercalation tracking does not provide direct information of the contribution of cell intercalation to tissue pure shear. Butler and colleagues in 2009 implemented a simple and effective method to measure the contribution of cell intercalation to pure shear in the prospective ectoderm of the *Drosophila* embryo [86]. Since tissue shear results from the sum of the integrated contributions of cell shear and cell intercalation, it is sufficient to measure tissue shear and the integrated contribution of cell shear and to subtract the first from the latter: this results in the integrated contribution of cell intercalation (figure 3). This method is very powerful since it relies on the measurement of only tissue and cell shear, which are computationally less demanding than any topological change measurement.

8. Conclusion and perspectives

Cell intercalation is implicated in numerous processes encompassing tissue morphogenesis in embryo gastrulation [5,8,9,24, 62,63,67], organogenesis [10,11,25–27,85,87], tissue homeostasis [1] and diseases (e.g. cancer cell invasion [4]). Understanding the fundamental mechanisms driving cell intercalation is thus of major importance.

The study of cell intercalation can be undertaken at different spatial and temporal scales. At a cellular resolution and at a time resolution of minutes, cell intercalation can be modelled by a quasi-steady-state distribution of cortical proteins and forces. Surface tension is predicted to increase with higher levels of cortical actomyosin and decrease with higher levels of E-cadherin-based adhesion. While such a model is powerful to eventually predict cellular packing and topology change, it remains a quite simplistic representation of reality. For example, E-cadherin clusters also act as anchoring sites without which actomyosin networks would not be able to generate contractile forces at the cell cortex. Actomyosin contractility and E-cadherin-based adhesion are thus interdependent. To provide a finer understanding of cell intercalation, analyses need to be carried out at a subcellular resolution and at a time resolution of seconds (i.e. the spatiotemporal resolution at which the dynamics of proteins and protein complexes are detectable) to bridge the gap between the cellular and the molecular level. At higher resolutions, pulses of actomyosin become visible. These pulses flow and eventually interact with the junctional cortex. Medial actomyosin pulses, beyond being under the control of upstream signalling factors (e.g. periodic upregulation/downregulation of the Rho pathway [42,43]), depend on the organization of the actomyosin network itself (e.g. F-actin and Myo II turnover rates, cross-linking proteins [45–47,88]). Actomyosin networks are dynamically coupled to the junctional cortex. Medial actomyosin pulses (e.g. via vincuilin) reinforce while cortical actomyosin (e.g. upregulating endocytosis [34]) weakens E-cadherin-based anchoring sites [50]. This results in a dynamic modulation of E-cadherin at the cell cortex [35,49,52]. While medial actomyosin networks asymmetrically coupled to the cortex can generate traction forces orienting actomyosin flows [48,49], actomyosin networks can flow independently of boundary anchoring conditions [47]. Polarized distribution of E-cadherin can modulate actomyosin network

properties (e.g. polarized fluidity) that can result in a self-sustained polarized flow [51].

Cell vertices are regions of high E-cadherin density where three or more cells are in proximity. During the first phase of cell intercalation (figure 1*a*, from (i) to (ii)), vertices appear to shift so that, on one side, one interface reduces in length while, on the other, two interfaces increase in length. Several hypotheses could explain how the process of simultaneous interface shortening and lengthening are coupled. One first hypothesis could be that the interface length change is driven by membrane trafficking (mediated for instance by endo/exocytosis). In this case, equal amounts of membrane need to be added or removed from both cells at a given interface to eventually drive coordinated interface lengthening or shortening, respectively. In addition, since interfaces radiating from the same vertex have equal rate of shortening/lengthening during vertex sliding, membrane trafficking has to be polarized and finely regulated so that membrane removal and addition rates are equal. E-cadherin proteins are modulated at vertices: low levels of E-cadherin correlate with vertex displacement but high levels with vertex stalling [52]. A second hypothesis could thus be that E-cadherin levels are regulated both at vertices and along interfaces to remodel contact junctions. A vertex could thus act as a membrane zipper: spot adherens junctions could be removed from the 'front' and new adhesion sites added at the 'back' of a sliding vertex. This would result in an apparent and simultaneous shortening and lengthening of interfaces. Photo-bleaching the membrane at the 'front' of a sliding vertex while monitoring vertex position using an E-cadherin fluorescent label could be an interesting experiment to validate one of the two hypothesis. For instance, if the photo-bleached membrane portion ends up being at the 'rear' of the vertex during vertex sliding, this would support the second hypothesis. Similar experiments would be informative to better decipher the extension of a new contact junction during the second phase of cell intercalation (figure 1*a*, from (iii) to (iv)). E-cadherin clusters at the cell junctional perimeters could play different roles depending on their specific location. E-cadherin clusters at vertices (together with vertex-specific adhesion complexes) could be key anchoring sites for the medial actomyosin network to exert traction forces for junction remodelling, while E-cadherin polarity at interfaces could direct actomyosin flows and eventual vertex sliding.

In recent years, outstanding work has advanced considerably our understanding of the force-based mechanisms driving cell intercalation. These mechanisms are tuned to provide reversible, irreversible, polarized or randomly oriented cell intercalations that can take place only at the interface between two competing cells, for instance, or throughout a tissue. Different intercalation dynamics and patterns can thus drive tissue morphogenesis, homeostasis or cell competition. We are now at a very exciting time when the knowledge of these fundamental mechanisms can be used to engineer new techniques to synthetically control tissue processes [69,89].

The first key epithelial transformations during early embryo development are elongation and folding. While the first process can separate the future head from the anus, the second can move a great number of cells to the inside of the embryo, where inner organs will form. Intercalation [8] and apical constriction [90] are key cellular processes driving tissue elongation and folding, respectively. Interestingly tissue extension and folding can take place along the same axis (for instance, during archenteron elongation in the sea urchin embryo [9]) or along orthogonal axes (for instance, during neurulation in the *X. laevis* embryo [82]). In the first case, tissue extension *per se* contributes to tissue folding. In the second case, extension and folding are orthogonal, thus *a priori* independent, processes. How can cells drive two simultaneous and independent processes? One possibility is that cells can simultaneously intercalate and apically constrict. If this is the case, how is the cytoskeletal machinery functioning to drive multiple cellular processes? In addition, what are the signalling factors controlling orthogonal tissue shape transformations? This is a new exciting riddle for future studies.

Data accessibility. This article has no additional data.

Competing interests. I declare that I have no competing interests.

Funding. This work was supported by the French government through the UCA^{JEDI} Investments in the Future project managed by the National Research Agency (ANR-15-IDEX-01), the 'Investments for the Future' LABEX SIGNALIFE (ANR-11-LABX-0028-01), the Tramplin ERC programme of the National Research Agency (ANR-16-TERC-0018-01), the ATIP-Avenir programme of the CNRS and the Human Frontier Science Program (CDA00027/2017-C).

References

1. Curran S, Strandkvist C, Bathmann J, De Gennes M, Kabla A, Salbreux G, Baum B. 2017 Myosin II controls junction fluctuations to guide epithelial tissue ordering. *Dev. Cell* **43**, 480–492. (doi:10.1016/j.devcel.2017.09.018)
2. Bi D, Lopez JH, Schwarz JM, Manning ML. 2014 Energy barriers and cell migration in densely packed tissues. *Soft Matter* **10**, 1885–1890. (doi:10.1039/c3sm52893f)
3. Marinari E, Mehonic A, Curran S, Gale J, Duke T, Baum B. 2012 Live-cell delamination counterbalances epithelial growth to limit tissue overcrowding. *Nature* **484**, 542–545. (doi:10.1038/nature10984)
4. Levayer R, Hauert B, Moreno E. 2015 Cell mixing induced by *myc* is required for competitive tissue invasion and destruction. *Nature* **524**, 476–480. (doi:10.1038/nature14684)
5. Firmino J, Rocancourt D, Saadaoui M, Moreau C, Gros J. 2016 Cell division drives epithelial cell rearrangements during gastrulation in chick. *Dev. Cell* **36**, 249–261. (doi:10.1016/j.devcel.2016.01.007)
6. Mongera A *et al.* 2018 A fluid-to-solid jamming transition underlies vertebrate body axis elongation. *Nature* **561**, 401–405. (doi:10.1038/s41586-018-0479-2)
7. Tetley RJ, Staddon MF, Heller D, Hoppe A, Banerjee S, Mao Y. 2019 Tissue fluidity promotes epithelial wound healing. *Nat. Phys.* **15**, 1195–1203. (doi:10.1038/s41567-019-0618-1)
8. Irvine KD, Wieschaus E. 1994 Cell intercalation during *Drosophila* germband extension and its regulation by pair-rule segmentation genes. *Development* **120**, 827–841.
9. Hardin JD, Cheng LY. 1986 The mechanisms and mechanics of archenteron elongation during sea urchin gastrulation. *Dev. Biol.* **115**, 490–501. (doi:10.1016/0012-1606(86)90269-1)
10. Sanchez-Corrales YE, Blanchard GB, Roper K. 2018 Radially patterned cell behaviours during tube budding from an epithelium. *eLife* **7**, e35717. (doi:10.7554/eLife.35717)
11. Sato K, Hiraiwa T, Maekawa E, Isomura A, Shibata T, Kuranaga E. 2015 Left–right asymmetric cell intercalation drives directional collective cell movement in epithelial morphogenesis. *Nat. Commun.* **6**, 10074. (doi:10.1038/ncomms10074)
12. Keller RE. 1980 The cellular basis of epiboly: an SEM study of deep-cell rearrangement during

gastrulation in *Xenopus laevis*. *J. Embryol. Exp. Morphol*. **60**, 201–234.

13. Warga RM, Kimmel CB. 1990 Cell movements during epiboly and gastrulation in zebrafish. *Development* **108**, 569–580.
14. McMahon A, Supatto W, Fraser SE, Stathopoulos A. 2008 Dynamic analyses of *Drosophila* gastrulation provide insights into collective cell migration. *Science* **322**, 1546–1550. (doi:10.1126/science.1167094)
15. Walck-Shannon E, Hardin J. 2014 Cell intercalation from top to bottom. *Nat. Rev. Mol. Cell Biol.* **15**, 34–48. (doi:10.1038/nrm3723)
16. Lecuit T, Lenne PF. 2007 Cell surface mechanics and the control of cell shape, tissue patterns and morphogenesis. *Nat. Rev. Mol. Cell Biol.* **8**, 633–644. (doi:10.1038/nrm2222)
17. Heisenberg CP, Bellaiche Y. 2013 Forces in tissue morphogenesis and patterning. *Cell* **153**, 948–962. (doi:10.1016/j.cell.2013.05.008)
18. Cavey M, Rauzi M, Lenne P, Lecuit T. 2008 A two-tiered mechanism for stabilization and immobilization of E-cadherin. *Nature* **453**, 751–756. (doi:10.1038/nature06953)
19. Yamada S, Pokutta S, Drees F, Weis WI, Nelson WJ. 2005 Deconstructing the cadherin-catenin-actin complex. *Cell* **123**, 889–901. (doi:10.1016/j.cell.2005.09.020)
20. Yonemura S, Wada Y, Watanabe T, Nagafuchi A, Shibata M. 2010 Alpha-catenin as a tension transducer that induces adherens junction development. *Nat. Cell Biol.* **12**, 533–542. (doi:10.1038/ncb2055)
21. Buckley CD, Tan J, Anderson KL, Hanein D, Volkmann N, Weis WI, Nelson WJ, Dunn AR. 2014 Cell adhesion. The minimal cadherin-catenin complex binds to actin filaments under force. *Science* **346**, 1254211. (doi:10.1126/science.1254211)
22. Engl W, Arasi B, Yap LL, Thiery JP, Viasnoff V. 2014 Actin dynamics modulate mechanosensitive immobilization of E-cadherin at adherens junctions. *Nat. Cell Biol.* **16**, 587–594. (doi:10.1038/ncb2973)
23. Nishimura T, Honda H, Takeichi M. 2012 Planar cell polarity links axes of spatial dynamics in neural-tube closure. *Cell* **149**, 1084–1097. (doi:10.1016/j.cell.2012.04.021)
24. Nishimura T, Takeichi M. 2008 Shroom3-mediated recruitment of Rho kinases to the apical cell junctions regulates epithelial and neuroepithelial planar remodeling. *Development* **135**, 1493–1502. (doi:10.1242/dev.019646)
25. Lienkamp SS, Liu K, Karner CM, Carroll TJ, Ronneberger O, Wallingford JB, Walz G. 2012 Vertebrate kidney tubules elongate using a planar cell polarity-dependent, rosette-based mechanism of convergent extension. *Nat. Genet.* **44**, 1382–1387. (doi:10.1038/ng.2452)
26. Karner CM, Chirumamilla R, Aoki S, Igarashi P, Wallingford JB, Carroll TJ. 2009 Wnt9b signaling regulates planar cell polarity and kidney tubule morphogenesis. *Nat. Genet.* **41**, 793–799. (doi:10.1038/ng.400)
27. Warrington SJ, Strutt H, Strutt D. 2013 The Frizzled-dependent planar polarity pathway locally promotes E-cadherin turnover via recruitment of RhoGEF2. *Development* **140**, 1045–1054. (doi:10.1242/dev.088724)
28. Kafer J, Hayashi T, Maree AFM, Carthew RW, Graner F. 2007 Cell adhesion and cortex contractility determine cell patterning in the *Drosophila* retina. *Proc. Natl Acad. Sci. USA* **104**, 18 549–18 554. (doi:10.1073/pnas.0704235104)
29. Farhadifar R *et al.* 2007 The influence of cell mechanics, cell-cell interactions, and proliferation on epithelial packing. *Curr. Biol.* **17**, 2095–2104. (doi:10.1016/j.cub.2007.11.049)
30. Rauzi M, Verant P, Lecuit T, Lenne P. 2008 Nature and anisotropy of cortical forces orienting *Drosophila* tissue morphogenesis. *Nat. Cell Biol.* **10**, 1401–1410. (doi:10.1038/ncb1798)
31. Bertet C, Sulak L, Lecuit T. 2004 Myosin-dependent junction remodelling controls planar cell intercalation and axis elongation. *Nature* **429**, 667–671. (doi:10.1038/nature02590)
32. de Matos Simões S, Blankenship JT, Weitz O, Farrell DL, Masako T, Fernandez-Gonzalez R, Zallen JA. 2010 Rho-kinase directs Bazooka/Par-3 planar polarity during *Drosophila* axis elongation. *Dev. Cell* **19**, 377–388. (doi:10.1016/j.devcel.2010.08.011)
33. Zallen JA, Wieschaus E. 2004 Patterned gene expression directs bipolar planar polarity in *Drosophila*. *Dev. Cell* **6**, 343–355. (doi:10.1016/S1534-5807(04)00060-7)
34. Levayer R, Pelissier-Monier A, Lecuit T. 2011 Spatial regulation of Dia and Myosin-II by RhoGEF2 controls initiation of E-cadherin endocytosis during epithelial morphogenesis. *Nat. Cell Biol.* **13**, 529–540. (doi:10.1038/ncb2224)
35. Rauzi M, Lenne PF, Lecuit T. 2010 Planar polarized actomyosin contractile flows control epithelial junction remodelling. *Nature* **468**, 1110–1114. (doi:10.1038/nature09566)
36. Sun Z, Amourda C, Shagirov M, Hara Y, Saunders T, Toyama Y. 2017 Basolateral protrusion and apical contraction cooperatively drive *Drosophila* germ-band extension. *Nat. Cell Biol.* **19**, 375–383. (doi:10.1038/ncb3497)
37. Munro E, Nance J, Priess JR. 2004 Cortical flows powered by asymmetrical contraction transport PAR proteins to establish and maintain anterior-posterior polarity in the early *C. elegans* embryo. *Dev. Cell* **7**, 413–424. (doi:10.1016/j.devcel.2004.08.001)
38. Skoglund P, Rolo A, Chen X, Gumbiner BM, Keller R. 2008 Convergence and extension at gastrulation require a myosin IIB-dependent cortical actin network. *Development* **135**, 2435–2444. (doi:10.1242/dev.014704)
39. Martin AC, Kaschube M, Wieschaus EF. 2009 Pulsed contractions of an actin–myosin network drive apical constriction. *Nature* **457**, 495–499. (doi:10.1038/nature07522)
40. Solon J, Colombelli J, Brunner D. 2009 Pulsed forces timed by a ratchet-like mechanism drive directed tissue movement during dorsal closure. *Cell* **137**, 1331–1342. (doi:10.1016/j.cell.2009.03.050)
41. He L, Wang X, Tang HL, Montell DJ. 2010 Tissue elongation requires oscillating contractions of a basal actomyosin network. *Nat. Cell Biol.* **12**, 1133–1142. (doi:10.1038/ncb2124)
42. Mason FM, Xie S, Vasquez CG, Tworoger M, Martin AC. 2016 RhoA GTPase inhibition organizes contraction during epithelial morphogenesis. *J. Cell Biol.* **214**, 603–617. (doi:10.1083/jcb.201603077)
43. Michaux JB, Robin F, Mcfadden WM, Munro EM. 2018 Excitable RhoA dynamics drive pulsed contractions in the early *C. elegans* embryo. *J. Cell Biol.* **217**, 4230–4252. (doi:10.1083/jcb.201806161)
44. Munjal A, Philippe J-M, Munro E, Lecuit T. 2015 A self-organized biomechanical network drives shape changes during tissue morphogenesis. *Nature* **524**, 351–355. (doi:10.1038/nature14603)
45. Senger F, Pitaval A, Ennomani H, Kurzawa L, Blanchoin L. 2019 Spatial integration of mechanical forces by α-actinin establishes actin network symmetry. *J. Cell Sci.* **132**, jcs236604. (doi:10.1242/jcs.236604)
46. Belmonte JM, Leptin M, Nedelec F. 2017 A theory that predicts behaviors of disordered cytoskeletal networks. *Mol. Syst. Biol.* **13**, 941. (doi:10.15252/msb.20177796)
47. Banerjee DS, Munjal A, Lecuit T, Rao M. 2017 Actomyosin pulsation and flows in an active elastomer with turnover and network remodeling. *Nat. Commun.* **8**, 1121. (doi:10.1038/s41467-017-01130-1)
48. Mori M, Monnier N, Daigle N, Bathe M, Ellenberg J, Lénárt P. 2011 Intracellular transport by an anchored homogeneously contracting F-actin meshwork. *Curr. Biol.* **21**, 606–611. (doi:10.1016/j.cub.2011.03.002)
49. Levayer R, Lecuit T. 2013 Oscillation and polarity of E-cadherin asymmetries control actomyosin flow patterns during morphogenesis. *Dev. Cell* **26**, 162–175. (doi:10.1016/j.devcel.2013.06.020)
50. Kale GR, Yang X, Philippe J-M, Mani M, Lenne P, Lecuit T. 2018 Distinct contributions of tensile and shear stress on E-cadherin levels during morphogenesis. *Nat. Commun.* **9**, 5021. (doi:10.1038/s41467-018-07448-8)
51. Pinheiro D *et al.* 2017 Transmission of cytokinesis forces via E-cadherin dilution and actomyosin flows. *Nature* **545**, 103–107. (doi:10.1038/nature22041)
52. Vanderleest TE, Smits CM, Xie Y, Jewett CE, Blankenship JT, Loerke D. 2018 Vertex sliding drives intercalation by radial coupling of adhesion and actomyosin networks during *Drosophila* germband extension. *eLife* **7**, e34586. (doi:10.7554/eLife.34586)
53. Weng M, Wieschaus E. 2016 Myosin-dependent remodeling of adherens junctions protects junctions from Snail-dependent disassembly. *J. Cell Biol.* **212**, 219–229. (doi:10.1083/jcb.201508056)
54. Blankenship JT, Backovic ST, Sanny J, Weitz O, Zallen JA. 2006 Multicellular rosette formation links planar cell polarity to tissue morphogenesis. *Dev. Cell* **11**, 459–470. (doi:10.1016/j.devcel.2006.09.007)

55. Chacon-Heszele MF, Ren D, Reynolds AB, Chi F, Chen P. 2012 Regulation of cochlear convergent extension by the vertebrate planar cell polarity pathway is dependent on p120-catenin. *Development* **139**, 968–978. (doi:10.1242/dev.065326)
56. Fernandez-Gonzalez R, de Matos Simoes S, Röper J-C, Eaton S, Zallen JA. 2009 Myosin II dynamics are regulated by tension in intercalating cells. *Dev. Cell* **17**, 736–743. (doi:10.1016/j.devcel.2009.09.003)
57. Collinet C, Rauzi M, Lenne P, Lecuit T. 2015 Local and tissue-scale forces drive oriented junction growth during tissue extension. *Nat. Cell Biol.* **17**, 1247–1258. (doi:10.1038/ncb3226)
58. Paré AC, Vichas A, Fincher CT, Mirman Z, Farrell DL, Mainieri A, Zallen JA. 2014 A positional Toll receptor code directs convergent extension in *Drosophila*. *Nature* **515**, 523–527. (doi:10.1038/nature13953)
59. Sulston JE, Schierenberg E, White JG, Thomson JN. 1983 The embryonic cell lineage of the nematode *Caenorhabditis elegans*. *Dev. Biol.* **100**, 64–119. (doi:10.1016/0012-1606(83)90201-4)
60. Williams-Masson EM, Heid PJ, Lavin CA, Hardin J. 1998 The cellular mechanism of epithelial rearrangement during morphogenesis of the *Caenorhabditis elegans* dorsal hypodermis. *Dev. Biol.* **204**, 263–276. (doi:10.1006/dbio.1998.9048)
61. Patel FB *et al.* 2008 The WAVE/SCAR complex promotes polarized cell movements and actin enrichment in epithelia during *C. elegans* embryogenesis. *Dev. Biol.* **324**, 297–309. (doi:10.1016/j.ydbio.2008.09.023)
62. Walck-Shannon E, Reiner D, Hardin J. 2015 Polarized Rac-dependent protrusions drive epithelial intercalation in the embryonic epidermis of *C. elegans*. *Development* **142**, 3549–3560. (doi:10.1242/dev.127597)
63. Munro EM, Odell GM. 2002 Polarized basolateral cell motility underlies invagination and convergent extension of the ascidian notochord. *Development* **129**, 13–24.
64. Keys DN, Levine M, Harland RM, Wallingford JB. 2002 Control of intercalation is cell-autonomous in the notochord of *Ciona intestinalis*. *Dev. Biol.* **246**, 329–340. (doi:10.1006/dbio.2002.0656)
65. Jiang D, Munro EM, Smith WC. 2005 Ascidian *prickle* regulates both mediolateral and anterior-posterior cell polarity of notochord cells. *Curr. Biol.* **15**, 79–85. (doi:10.1016/j.cub.2004.12.041)
66. Oda-Ishii I, Ishii Y, Mikawa T. 2010 Eph regulates dorsoventral asymmetry of the notochord plate and convergent extension-mediated notochord formation. *PLoS ONE* **5**, e13689. (doi:10.1371/journal.pone.0013689)
67. Shih J, Keller R. 1992 Cell motility driving mediolateral intercalation in explants of *Xenopus laevis*. *Development* **116**, 901–914.
68. Guglielmi G, Barry JD, Huber W, De Renzis S. 2015 An optogenetic method to modulate cell contractility during tissue morphogenesis. *Dev. Cell* **35**, 646–660. (doi:10.1016/j.devcel.2015.10.020)
69. Izquierdo E, Quinkler T, De Renzis S. 2018 Guided morphogenesis through optogenetic activation of Rho signalling during early *Drosophila* embryogenesis. *Nat. Commun.* **9**, 2366. (doi:10.1038/s41467-018-04754-z)
70. Krueger D, Tardivo P, Nguyen C, De Renzis S. 2018 Downregulation of basal myosin-II is required for cell shape changes and tissue invagination. *EMBO J.* **37**, e100170. (doi:10.15252/embj.2018100170)
71. Szabo A, Cobo I, Omara S, Mclachlan S, Keller R, Mayor R. 2016 The molecular basis of radial intercalation during tissue spreading in early development. *Dev. Cell* **37**, 213–225. (doi:10.1016/j.devcel.2016.04.008)
72. Shindo A, Wallingford JB. 2014 PCP and septins compartmentalize cortical actomyosin to direct collective cell movement. *Science* **343**, 649–652. (doi:10.1126/science.1243126)
73. Shindo M, Wada H, Kaido M, Tateno M, Aigaki T, Tsuda L, Hayashi S. 2008 Dual function of Src in the maintenance of adherens junctions during tracheal epithelial morphogenesis. *Development* **135**, 1355–1364. (doi:10.1242/dev.015982)
74. Shindo A. 2018 Models of convergent extension during morphogenesis. *WIREs Dev. Biol.* **7**, e293. (doi:10.1002/wdev.293)
75. Yu JC, Fernandez-Gonzalez R. 2016 Local mechanical forces promote polarized junctional assembly and axis elongation in *Drosophila*. *eLife* **5**, e10757. (doi:10.7554/eLife.10757)
76. Bardet PL *et al*. 2013 PTEN controls junction lengthening and stability during cell rearrangement in epithelial tissue. *Dev. Cell* **25**, 534–546. (doi:10.1016/j.devcel.2013.04.020)
77. Finegan TM, Hervieux N, Nestor-Bergmann A, Fletcher AG, Blanchard GB, Sanson B. 2019 The tricellular vertex-specific adhesion molecule Sidekick facilitates polarised cell intercalation during *Drosophila* axis extension. *PLoS Biol.* **17**, e3000522. (doi:10.1371/journal.pbio.3000522)
78. Letizia A, He DQ, Astigarraga S, Colombelli J, Hatini V, Llimargas M, Treisman JE. 2019 Sidekick is a key component of tricellular adherens junctions that acts to resolve cell rearrangements. *Dev. Cell* **50**, 313–326. (doi:10.1016/j.devcel.2019.07.007)
79. Uechi H, Kuranaga E. 2019 The tricellular junction protein Sidekick regulates vertex dynamics to promote bicellular junction extension. *Dev. Cell* **50**, 327–338. (doi:10.1016/j.devcel.2019.06.017)
80. Condic ML, Fristrom D, Fristrom JW. 1991 Apical cell shape changes during *Drosophila* imaginal leg disc elongation: a novel morphogenetic mechanism. *Development* **111**, 23–33.
81. Gomez-Galvez P *et al.* 2018 Scutoids are a geometrical solution to three-dimensional packing of epithelia. *Nat. Commun.* **9**, 2960. (doi:10.1038/s41467-018-05376-1)
82. Keller R. 2002 Shaping the vertebrate body plan by polarized embryonic cell movements. *Science* **298**, 1950–1954. (doi:10.1126/science.1079478)
83. Behrndt M, Salbreux G, Campinho P, Hauschild R, Oswald F, Roensch J, Grill SW, Heisenberg C-P. 2012 Forces driving epithelial spreading in zebrafish gastrulation. *Science* **338**, 257–260. (doi:10.1126/science.1224143)
84. Rauzi M, Krzic U, Saunders TE, Krajnc M, Ziherl P, Hufnagel L, Leptin M. 2015 Embryo-scale tissue mechanics during *Drosophila* gastrulation movements. *Nat. Commun.* **6**, 8677. (doi:10.1038/ncomms9677)
85. Aigouy B *et al.* 2010 Cell flow reorients the axis of planar polarity in the wing epithelium of *Drosophila*. *Cell* **142**, 773–786. (doi:10.1016/j.cell.2010.07.042)
86. Butler LC, Blanchard GB, Kabla AJ, Lawrence NJ, Welchman DP, Mahadevan L, Adams RJ, Sanson B. 2009 Cell shape changes indicate a role for extrinsic tensile forces in *Drosophila* germ-band extension. *Nat. Cell Biol.* **11**, 859–864. (doi:10.1038/ncb1894)
87. Wang J *et al.* 2005 Regulation of polarized extension and planar cell polarity in the cochlea by the vertebrate PCP pathway. *Nat. Genet.* **37**, 980–985. (doi:10.1038/ng1622)
88. Jodoin JN, Coravos JS, Chanet S, Vasquez CG, Tworoger M, Kingston ER, Perkins LA, Perrimon N, Martin AC. 2015 Stable force balance between epithelial cells arises from F-actin turnover. *Dev. Cell* **35**, 685–697. (doi:10.1016/j.devcel.2015.11.018)
89. Baillie-Johnson P, van den Brink SC, Balayo T, Turner DA, Arias AM. 2015 Generation of aggregates of mouse embryonic stem cells that show symmetry breaking, polarization and emergent collective behaviour *in vitro*. *J. Vis. Exp.* **105**, 53252. (doi:10.3791/53252)
90. Leptin M, Grunewald B. 1990 Cell shape changes during gastrulation in *Drosophila*. *Development* **110**, 73–84.